$Ag_{50}(Dppm)_6(SR)_{30}$ and its homolog $Au_xAg_{50-x}(Dppm)_6(SR)_{30}$ alloy nanocluster: Seeded Growth, Structure Determination and Differences of Properties

Wenjun Du,[†,‖] Shan Jin,[†,‖] Lin Xiong,[‡] Man Chen,[†] Jun Zhang,[§] Xuejuan Zou,[†] Yong Pei,[‡] Shuxin Wang,[*,†] and Manzhou Zhu[*,†]

[†]Department of Chemistry and Center for Atomic Engineering of Advanced Materials, Anhui University, Hefei, Anhui 230601, People's Republic of China

[‡]Department of Chemistry, Key Laboratory of Environmentally Friendly Chemistry and Applications of Ministry of Education, Xiangtan University, Xiangtan, Hunan 411105, People's Republic of China

[§]School of Materials and Chemical Engineering, Anhui Jianzhu University, Hefei, Anhui 230601, People's Republic of China

Supporting information:

Crystal data for $Ag_{50}(Dppm)_6(SR)_{30}$ nanocluster. Space group $P\bar{1}$, a = 26.2512(12) Å, b = 26.6936(12) Å, c = 26.7376(12) Å, α = 76.576(2)°, β = 60.718(2)°, γ = 61.726(2)°, V = 14392.3(12) Å^3, T = 150(2) K, Z = 1, 206755 reflections measured, 53140 unique reflections (R_{int}=0.0596), final R_1 = 0.0619 and wR_2 = 0.1606 for ($I > 2\sigma(I)$).

Crystal data for $Ag_xAu_{50-x}(Dppm)_6(SR)_{30}$ nanocluster. Space group $P\bar{1}$, a = 25.8780(9) Å, b = 26.0327(9) Å, c = 26.5129(9) Å, α = 61.613(2)°, β = 75.949(2)°, γ = 61.416(2)°, V = 13795.5(8) Å^3, T = 150(2) K, Z = 1, 183433 reflections measured, 50714 unique reflections (R_{int}=0.0731), final R_1 = 0.1497 and wR_2 = 0.3478 for ($I > 2\sigma(I)$).

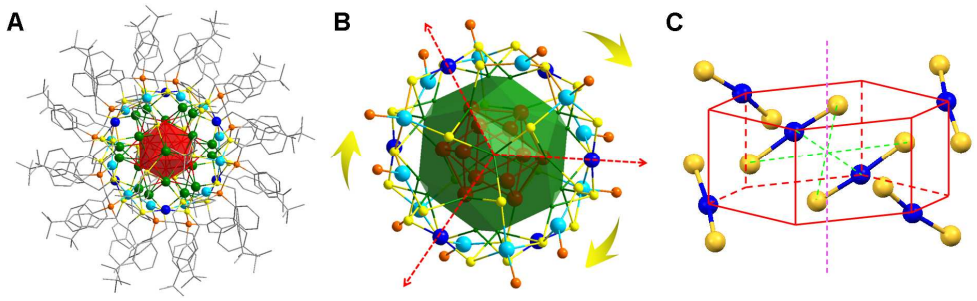

Figure S1. (A) the total structure of the $M_{5.34}Ag_{44.66}(Dppm)_6(SR)_{30}$ (M=Au/Ag) nanocluster.; (B) the trigonal axis (C_3) of $M_{5.34}Ag_{44.66}(Dppm)_6(SR)_{30}$ (M=Au/Ag) nanocluster; (C) the arrangement of the six "S-Ag-S" staples formed a hexagonal prism, and made the $M_{5.34}Ag_{44.66}(Dppm)_6(SR)_{30}$ (M=Au/Ag) nanocluster a S_6/C_{3i} point group.(color labels: red/green/blue/sky blue=Ag; yellow=S; orange=P; gray=C)

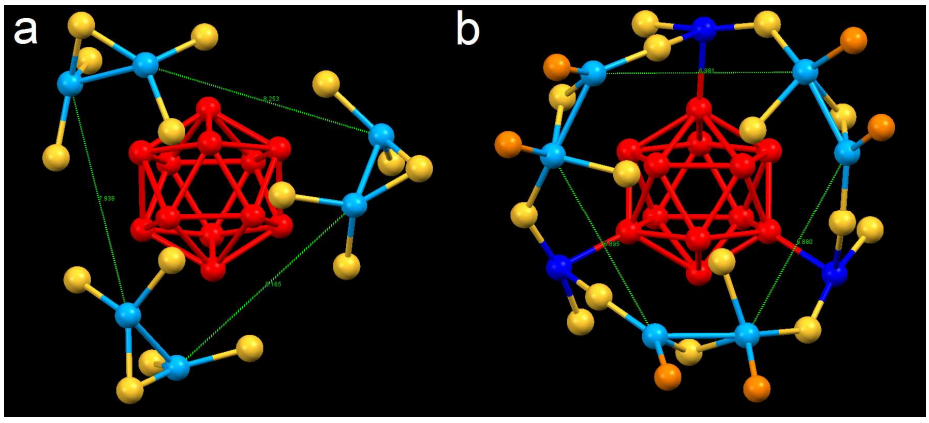

Figure S2. The comparison of the structures of different surface staple units between $Ag_{44}(SR)_{30}^{4-}$ and $Ag_{50}(Dppm)_6(SR)_{30}$ (color labels: red/blue/sky blue=Ag; yellow=S; orange=P)

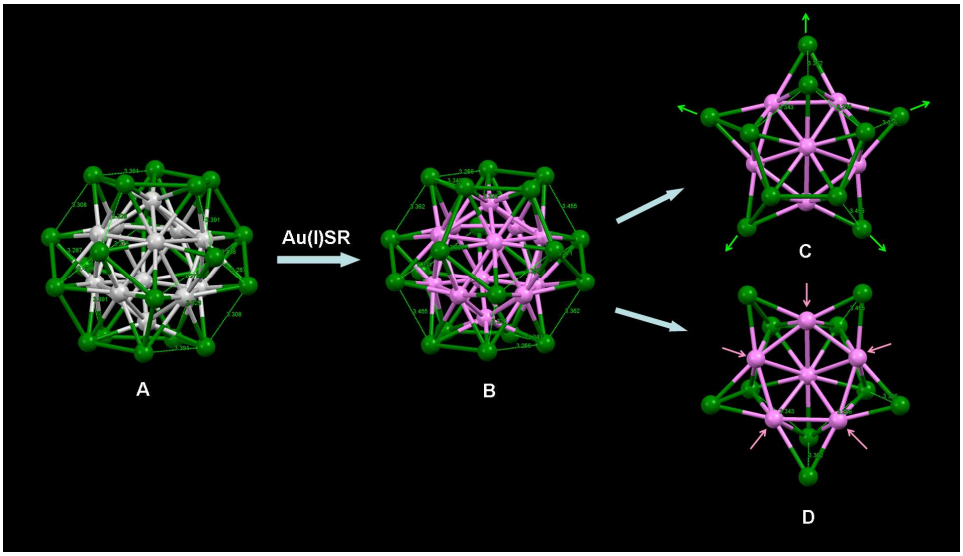

Figure S3. The M_{32} kernel structure of (A) the $Ag_{50}(Dppm)_6(SR)_{30}$ and (B) the $Au_{5.34}Ag_{44.66}(Dppm)_6(SR)_{30}$. (C) The top view of the half of the M_{32} kernel of the $Au_{5.34}Ag_{44.66}(Dppm)_6(SR)_{30}$ shows that the Ag_{20} kernel of $Au_{5.34}Ag_{44.66}$ is bigger than the Ag_{50}; (D) The bottom view of the half of the M_{32} kernel of the $Au_{5.34}Ag_{44.66}(Dppm)_6(SR)_{30}$ shows that the Ag_{12} core of $Au_{5.34}Ag_{44.66}$ is smaller than the Ag_{50} (color labels: silver/ green=Ag; violet=Ag/Au)

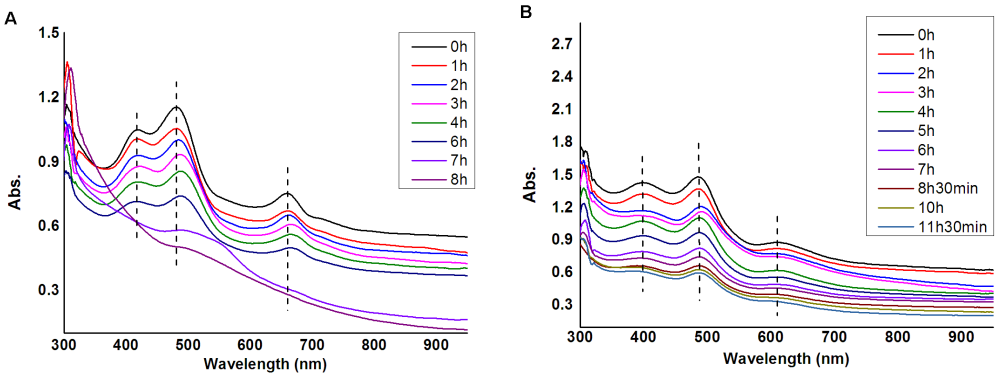

Figure S4. Time dependent UV-Vis spectra of (a) $Ag_{50}(Dppm)_6(SR)_{30}$ and (b) $Au_{5.34}Ag_{44.66}(Dppm)_6(SR)_{30}$ heated in methanol solution at 50° C. $Au_{5.34}Ag_{44.66}(Dppm)_6(SR)_{30}$ clusters exhibit a much higher stability than $Ag_{50}(Dppm)_6(SR)_{30}$.

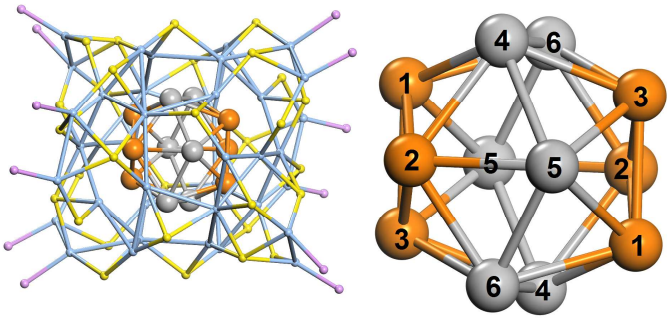

Sites	Ag%	Au%	Total Ag	Total Au
1	54.170%	45.830%		
2	53.105%	46.895%		
3	54.231%	45.769%		
4	56.215%	43.785%		
5	57.340%	42.660%		
6	57.891%	42.109%		
			6.659	5.341

Figure S5. The details of the Au occupied atoms in the M_{12} core of $Au_xAg_{50-x}(Dppm)_6(SR)_{30}$ (M=Au/Ag) (color labels: sky blue=Ag; yellow=S; violet=P; silver= Ag/ Au; brown=Au/Ag).

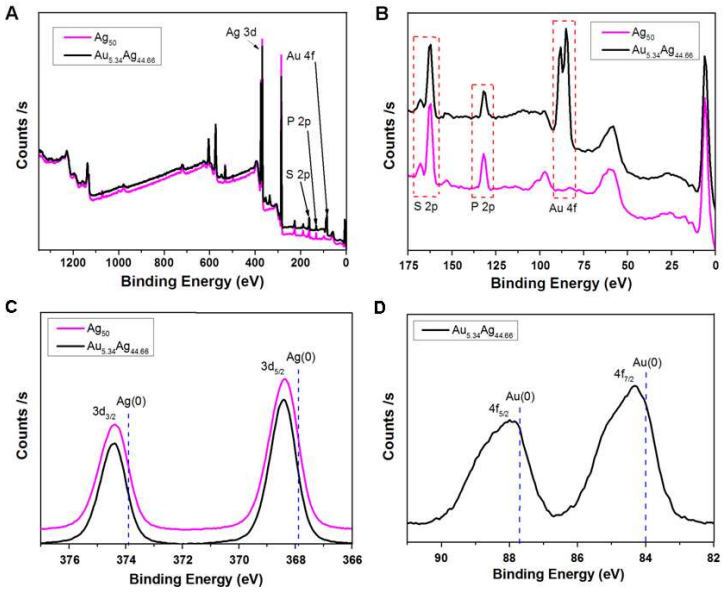

Figure S6. The XPS data of the $M_{5.34}Ag_{44.66}(Dppm)_6(SR)_{30}$ (M=Au/Ag) nanoclusters: (A) is the survey data, (B) is the details data of the S 2p, P 2p and Au 4f region, (C) is the Ag 3d region of $M_{5.34}Ag_{44.66}(Dppm)_6(SR)_{30}$ (M=Au/Ag) nanoclusters and bulk Ag (the blue line in C), and (D) is the region of $Au_{5.34}Ag_{44.66}(Dppm)_6(SR)_{30}$ and bulk Au (the blue line in D).

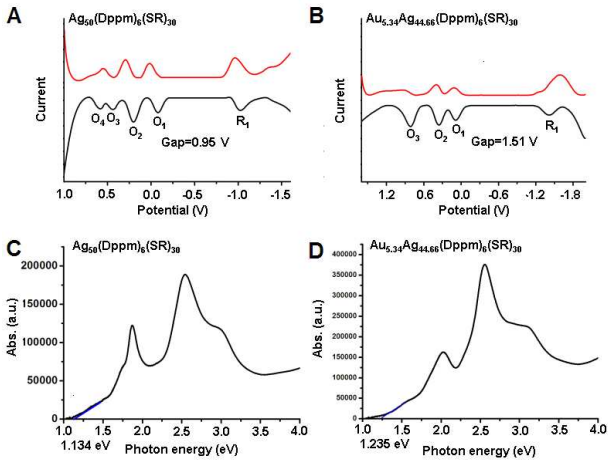

Figure S7. The DPVs and photon energies of the $M_{5.34}Ag_{44.66}(Dppm)_6(SR)_{30}$ (M=Au/Ag) nanoclusters: (A) is the DPV of $Ag_{50}(Dppm)_6(SR)_{30}$ with a gap of 0.95 V, (B) is the DPV of $Au_{5.34}Ag_{44.66}(Dppm)_6(SR)_{30}$ with a gap of 1.51 V, (C) is the photon energy of $Ag_{50}(Dppm)_6(SR)_{30}$ with a gap of 1.134 eV, and (D) is the photon energy of $Au_{5.34}Ag_{44.66}(Dppm)_6(SR)_{30}$ with a gap of 1.235 eV.

Table S1. Summary peak heights of ESI-MS.

molecular formula	peak height	proportion	total
$Au_4Ag_{46}(Dppm)_6(SR)_{30}$	613.04	0.129	
$Au_5Ag_{45}(Dppm)_6(SR)_{30}$	1872.90	0.395	
$Au_6Ag_{44}(Dppm)_6(SR)_{30}$	1927.98	0.407	
$Au_7Ag_{43}(Dppm)_6(SR)_{30}$	325.95	0.069	
			$Au_{5.42}Ag_{44.58}(Dppm)_6(SR)_{30}$

Table S2. Summary of XPS data; all values are in eV.

	Ag $3d_{3/2}$	**Ag $3d_{5/2}$**	**Au $4f_{5/2}$**	**Au $4f_{7/2}$**
Bulk Ag	373.9	367.9	--	--
Bulk Au	--	--	87.7	84.0
$Ag_{50}(Dppm)_6(SR)_{30}$	374.43	368.42	--	--
$Au_{5.34}Ag_{44.66}(Dppm)_6(SR)_{30}$	374.45	368.44	87.95	84.30

Table S3. The hirshfeld charge analysis (in units of |e|) of Ag(Au), S and P atoms in $Ag_{50}(Dppm)_6(SR)_{30}$ and $Au_6Ag_{44}(Dppm)_6(SR)_{30}$

	Kernel	Ag_{20}	Ag_{18}	S	P
Ag_{50}	0.098	1.649	2.019	-3.688	2.010
Au_6Ag_{44}	-0.077	1.792	1.978	-3.664	2.013

Table S4. The hirshfeld charge analysis (in units of |e|) of kernel in $Ag_{50}(Dppm)_6(SR)_{30}$ and $Au_6Ag_{44}(Dppm)_6(SR)_{30}$ clusters.

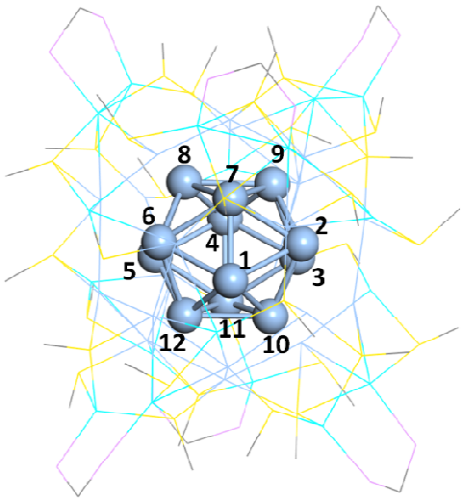

$Ag_{50}(Dppm)_6(SR)_{30}$

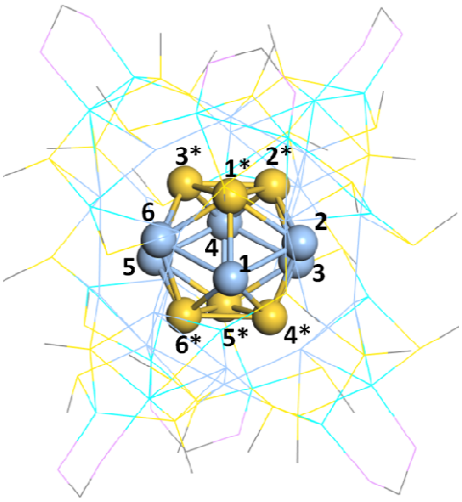

$Au_6Ag_{44}(Dppm)_6(SR)_{30}$

Ag_{50}	**1**	**2**	**3**	**4**	**5**	**6**	7	8	9	10	11	12
	0.008	**0.007**	**0.008**	**0.008**	**0.007**	**0.007**	0.010	0.011	0.008	0.008	0.009	0.007
Au_6Ag_{44}	**1**	**2**	**3**	**4**	**5**	**6**	1*	2*	3*	4*	5*	6*
	0.017	**0.018**	**0.017**	**0.018**	**0.017**	**0.018**	-0.031	-0.031	-0.030	-0.030	-0.030	-0.030